Techno-economic evaluation of the performance of an innovative rotary disk receiver concept in a CSP power plant

Cite as: AIP Conference Proceedings **2445**, 110010 (2022); https://doi.org/10.1063/5.0085715
Published Online: 12 May 2022

Xabier Rández, Fritz Zaversky and David Astrain

Techno-Economic Evaluation of the Performance of an Innovative Rotary Disk Receiver Concept in a CSP Power Plant

Xabier Rández[1, a)], Fritz Zaversky[1] and David Astrain[2]

[1]*National Renewable Energy Center of Spain (CENER), Solar Thermal Energy and Thermal Storage Department. Av. Ciudad de la Innovación, 7, 31621 Sarriguren,(Navarre), Spain*
[2]*Public University of Navarre (UPNA), Department of Engineering, Pamplona, Navarre, Spain*

[a)]Corresponding author: xrandez@cener.com

Abstract. This study evaluates the thermal performance of an innovative discs receiver and models its effect in a CSP plant. Energetic and economic results were compared with a foam receiver developed in the European project CAPTure. The study consists of two parts, on the one hand, it treats the simulation of a CFD model of the innovative disk receiver, from which the thermal efficiency versus air outlet temperature curve was obtained, necessary to feed the second part of the study. This thermal efficiency was compared with the performance of a foam receiver. On the other hand, system-level simulations of a CSP multi tower plant are performed in order to obtain the effect of this efficiency-air outlet temperature curve on the overall energetic and economic performance. The study compares the LCOE and the yearly generation of the plant with the innovative discs receiver with that of the foam receiver. Results show the potential in economic and energetic terms of the new receiver in comparison to conventional foam receivers.

INTRODUCTION

The increasing problems with global warming and energy generation have reinforced the interest in renewable sources of energy. Concentrated solar power (CSP) is a renewable energy which harnesses the solar radiation incident on planet earth in order to generate electricity. CSP plants concentrate the sun's direct normal irradiance (DNI) onto a receiving surface and transfer the absorbed heat to a high temperature fluid stream, which, at a later stage, powers a conventional thermodinamic power cycle, in order to generate electricity. CSP is a highly promising alternative to fossil fuel technology as solar thermal power plants can provide dispatchable power by thermal energy storage or by hybridization with biomass or gas. Today, the parabolic through collector is the most extended technology with solar-to-electric conversion efficiencies not higher than 15% on an annual basis [1]. This limit in conversion is due to the limited operating temperature (400 °C) defined by the heat transfer fluid (HTF) [2].

The power tower concept, on the contrary, allows to achieve higher efficiencies by using molten salts or air as HTF [3] and higher concentration ratios on the receiver's surface [4]. The solar absorber or receiver is a key component in this technology and its design and configuration depends on the HTF applied. For the case of air as HTF, which is a promising candidate for high-temperature applications as it has no temperature limitations, open volumetric air receivers (OVARs) have shown good performance [5].

The development of volumetric receivers started in Germany in the eighties and its design has not changed much since then. Conventional volumetric receivers are usually formed by foams or honeycomb structures based on prismatic channels (see Fig. 1) where radiation is absorbed and transfered to the air [6] or foam absorbers.

The volumetric receiver's thermal efficiency is usually better than that of conventional tubular receivers, due to the so-called volumetric effect. Volumetric receivers are made of metal or ceramic materials and porous geometry so that the radiation is absorbed in the depth of the receiver [7]. The solar radiation heats the volume of the absorber and the heat transfer fluid, usually air, passes through the absorber and it is warmed up by convection [8].

SolarPACES 2020
AIP Conf. Proc. 2445, 110010-1–110010-8; https://doi.org/10.1063/5.0085715
Published by AIP Publishing. 978-0-7354-4195-8/$30.00

Volumetric receivers can operate in two ways: open loop and closed loop. In open loop receiver systems, atmospheric air is heated up through a receiver and then used to generate high preassure steam in a heat exchanger. This steam feeds a Rankine turbine generator system. In closed loop receiver systems, pressurized air is heated in a cavity and then fed into a gas turbine of a Brayton Cycle [6] [9]. As an alternative concept, recent developments have proposed the application of a high-temperature air/air heat exchanger in order to power the Brayton Cylce externally by using an atmospheric air HTF primary loop powered by OVARs, also integrating thermal energy storage upstream the gas turbine [10].

FIGURE 1. Conventional cup

In the context of solar powered combined cycles [11], the thermal efficiency of the OVAR has shown to be a key parameter for the power plant's overall solar-to-electric conversion efficiency and thus economic viability.

With the motivation to improve the receiver's thermal performance, this work focuses on the techno-economic analysis of an innovative rotary disk volumetric receiver concept as presented in [12].

The new receiver design is composed of a group of disks that rotate with a shaft. The shaft is assembled inside a ceramic cup with square shape. The main concept of the rotating disk is to transport the heat from the frontal receiver face to interior zones into the cavity. This design ensures homogeneous heating of the ceramic structure and improves the convective heat transfer between disks and air. Also, due to the active movement of the absorber and better heat removal, stable operation under higher flux densities (higher concentration ratios) is expected.

Figure 2 (a) shows a 3D view of the laboratory scale prototype (aperture size: 3 x 3 cm). The figure presents the cavity and the disks. It can be seen that the aperture of the top and the bottom shape of the cavity is adapted to the disks' shape in order to improve thermal efficiency. Note that in upscaled configuration (cup aperture size of 14 x 14 cm), the disk package may protrude from the cup's aperture plane and a frame made of ceramic foam may cover the front edges of the cup, in order to protect the cup from incident solar flux. Such a design would be a hybrid configuration, combinig the classical fixed foam absorber concept with the innovative rotary disk approach (see Fig. 2 (b)).

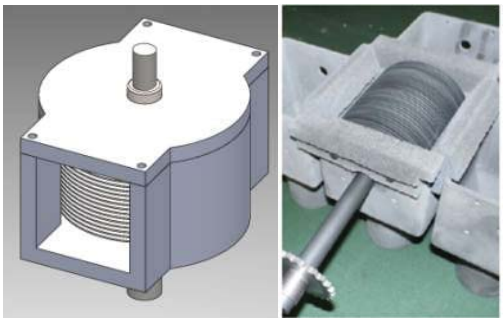

a) b)

FIGURE 2. Receiver 3D model (a) and prototype (b) [12]

METHODOLOGY

As mentioned above, the whole study is carried out in two sequential stages. First, a receiver CFD model validated at laboratory scale estimates the thermal performance of the receiver. Then, the temperature and thermal

efficiency results obtained in CFD simulations were implemented in a system-level CSP plant model in order to know the LCOE and yearly generation of the plant with the discs receiver. All these results, obtained from receiver CFD model and from the CSP plant model were compared with the obtained results for a foam receiver (Fig. 3) in the project CAPTure.

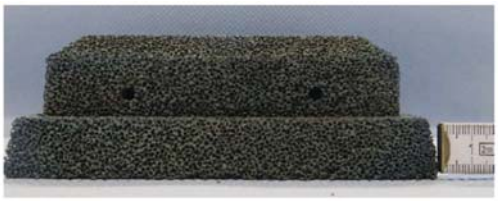

FIGURE 3. Foam absorber [12]

Receiver CFD Model

The computational domain is composed of a group of thin disks that rotates clockwise around y axes and the air stream wich flows in xz plane through the receiver cavity.

The modeling of completely prototype requires a too big 3-D mesh in terms of number of elements, with unreasonable computational cost. Due to this, it is necessary simplify the model to reduce number of elements below acceptable values. The symmetry in the geometry of the receiver allows to reduce in a half the size of the model. The shaft is also erased in order to simplify the geometry of the model and improve the convergence. By last, the external walls of the receiver are considered adiabatic and removed from the simulation to reduce the computational cost. This simplification is correct only if the walls are thermally insulated as in this case.

Figure 4 shows the 3D geometry simulated in the model. ANSYS Fluent is the commercial CFD software based on finite elements. It is difficult to represent accurately the boundary layer between the disks. The mesh around the disks must be fine enough to solve the thermal and viscous gradients, which are pronounced near the disk surfaces. In Fig. 4 b can be seen the detailed mesh near the surfaces of the disks. The fluid mesh is refined as it approaches the disc surface to accurately resolve the thermal boundary layer.

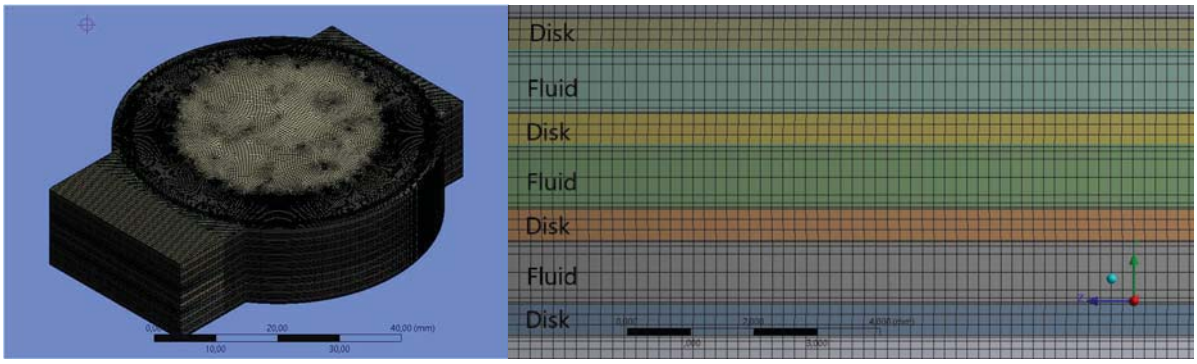

FIGURE 4. Fluent 3D mesh

Navier-Stokes, energy and radiation transport equations were numerically solved with Fluent code from ANSYS. The numerical solution of governing equations was performed with the "pressure-based" approach, which assumes that mass density depends on temperature and on a fixed pressure reference value [13]. The SIMPLE (Semi-Implicit Method for Pressure-Linked Equations) algorithm [14][15] was used as pressure-velocity coupling scheme. Most of numerical studies of solar receivers [5][7][8] used LES with dynamic Smagorinsky aproach as turbulence model but in this case, the high number of elements of the model translates in an unacceptable computational cost. Furthermore, LES model is inherently transient and the main interest of this study is the steady state. RANS turbulence models were taken into account at the time to select the optimal turbulence model. The selecting turbulence model criteria was the accuracy of solution obtained by the simulation of a disk in a wind tunel, like previous studies. Simulations shows that k-ω SST model provides better results than other models like standard k-ω or k-ε. Furthermore, the suitability of this model for a rotating object in an air flow has been widely studied in several previous investigations [16][17][18].

The k-ω SST model combines k-ω and k-ε models depending on the distance with the walls. In zones where the flow is near to a wall, k-ω model describes better the flow development; by contrast, k-ε model is suited in zones with free stream flow [19]. Values for y+ were below 10 for surfaces of the disks in contact with the air flow.

In Fig 4 is shown the case of study in wich a group of 10 thin disks rotates around y axes and the air stream blows perpendicular to y-x plane. The computational domain is composed of 10 thin disks and the air inside the receiver cavity. Receiver external walls are adiabatic and do not contribute to final simulation result in steady mode. The midpoint of the receivers frontal face is placed in the origin of the Cartesian system of coordinate.

The air stream blows uniformly through the receiver from the frontal face to the rear face with the velocity vector of $\vec{V} = 0\vec{\imath} + 0\vec{\jmath} + u_{in}\vec{k}$ and the temperature of $T = T_{\infty}$ in the inlet face. Rotation of the flow and the disks was modeled by using the moving reference frame; moving reference frame allows solve a model which is inertial with respect to the moving frame. For a steadily rotating body, it is possible to transform the equations of fluid motion to the rotating frame solving it as steady-state problem [13]. Air flow is defined in boundary conditions like velocity inlet, in the inlet face of receiver, and outflow, in the outlet face of receiver, in order to improve model convergence.

The disks are composed of 2 parts, a smaller disk and a thin ring which simultaneously rotate as a single element. This separation into two parts is due to the modelling of the solar flux on the disks as a volumetric source in the solid phase (on the surface), the thin ring. The size of the ring was determined by optical simulations and is equal to the deph reached by solar radiation. The optical simulations has been carried out with a ray tracing software, Tonatiuh, based in Monte Carlo method. Two disks are placed in the focus of a parabollic disk concentrator and the penetration deph of light rays has been calculated. The use of a volumetric source on the surface of a solid is a widely known and used method in the modeling of surface heat fluxes like in this case [14].

The solar flux is constant and uniform in the entire frontal face. The performance of the receiver were evaluated for DNI from 600 kW/m^2 to 1000 kW/m^2. This radiative flux is introduced in the CFD model as a heat generation by an user defined function applied to the thin ring, the user defined function limits the heat generation in the ring within the boundaries defined by the receiver aperture. The UDF has been calculated by using the radiation heat flux, the complete area exposed to solar radiation and the global and element volumes. The radiative heat transfer between the disks, the inner walls of the cavity and the ambient has been modeled using the surface to surface model (S2S). This model assumes that the surfaces in the model are grey and difusse.

The complete model mesh is built by more than $6{\cdot}10^6$ elements in the shape of rectangular prisms. To increase the accuracy of the convective results, the grid size is finer near the walls of the disks and in the gap between the disks. The impact of the grid on the accuracy of the results is corrobotated in the outlet temperature and mean Nusselt results with 6 different meshes. Meshes with number of elements above $7{\cdot}10^6$ provides results that are independent of the grid size.

The rotating disks material is silicon carbide and its properties are defined in Fluent as temperature dependent in the case of specific heat and as fixed for the rest of the properties; this fixed properties are defined at working temperature (1000 °C).The air properties are also defined as temperature dependent. Table 1 shows the material properties introduced in Fluent.

TABLE 1. Material properties in CFD model

Parameter	Parameter
SiC Absorptance α	0.8
SiC Density	3100 kg/m^3
SiC Thermal Conductivity	Table with K depending on temperature between 373K and 1373K
SiC Emittance E	0.83
SiC Cp	Table with Cp depending on temperature between 473K and 1773K
Air Density	Ideal Gas density from Fluent Database
Air Cp	Table with Cp depending on temperature between 200K and 2150K
Air Dynamic Viscosity	$\mu\left(\frac{kg}{s*m}\right) = -1.709*10^{-11}T^2 + 5.630*10^{-8}T + 3.009*10^{-6}$
Air Thermal Conductivity	$k\left(\frac{W}{m*K}\right) = 1.582*10T^3 - 5.666*10^{-8}T^2 + 1.090*10^{-4}T - 0.00169$

CSP Plant Model

The system-level CSP plant model replicates the behavior of a solar-only-powered combined cycle plant, applying two models: the model of the solar-to-thermal energy conversion process and the model of the power cycle, i.e. the thermal-to-electric energy conversion process. The resulting solar-to-electric efficiency, or simply solar efficiency, is the product of solar-to-thermal efficiency and thermal-to-electric efficiency. The plant configuration chosen for this evaluation is a multi-tower central receiver power plant with six towers, having each about 51 MW nominal solar power (north fields) [20]. This model was built in Dymola using Modelica language [20].

The efficiency of the solar part depends on the receiver efficiency, which is obtained in the previous step of the study, and the optical efficiency, which depends on the heliostat field. In order to offer the full performance potential for the heliostat field, in this work only compact multi-tower heliostat fields with a peak optical efficiency of about 0.8 are taken into account, which is very likely to be the field design of next generation power tower plants, as compact heliostat fields provide significantly better efficiencies and better solar flux control. The final heliostat field is thus an array of 6 identical subfields (306 MW total nominal solar power). When increasing the number of towers, the HTF transport tends to become an issue. The model of the solar-to-thermal energy conversion process is composed of the receiver performance matrix, depending on air outlet temperature and solar DNI, and the matrix-based heliostat field model obtained via a series of ray tracing simulations in Tonatiuh (see [20]).

For the thermal-to-electric part, a combined cycle plant with reheated Brayton cycle and TES has been modeled. Fig. 5 shows the scheme of the combined cycle configuration analyzed; as it can be seen, the detailed tube bundle and steam drum configuration of the heat recovery steam generator (HRSG), as well as Rankine cycle architecture is not shown for the sake of simplicity.

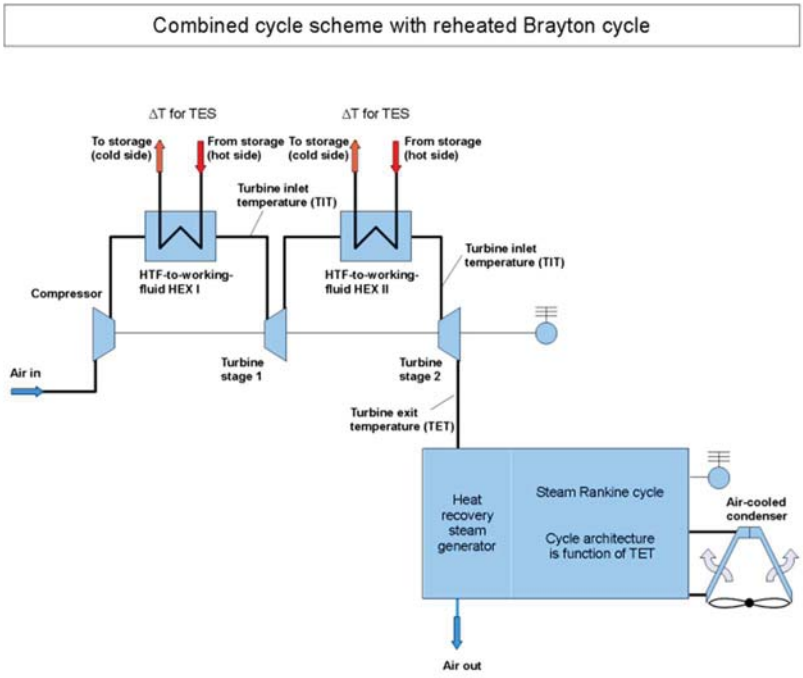

FIGURE 5. Combined cycle scheme **[20]**

The modeling of the combined cycle is described in detail in Ref [20]. The modeling of the un-cooled gas turbine is straight forward and applies simple isoentropic relationships for an ideal gas. Simulation results of the Brayton cycle part have been checked against other software packages [21] [22]. The bottoming Rankine cycle performance has been estimated applying state-of-the-art power cycle simulation software [21] and generating performance tables as function of HRSG inlet temperature and ambient temperature [22], suitable for annual yield simulations. The

annual plant performance parameters (i.e. electricity yield, annual solar-to-electric efficiency) have been obtained running annual energy yield simulations using a typical meteorological year for Seville, Spain.

The financial model LCOE has been developed according to Ref. [23]. The high uncertainties related to cost assumptions must be taken into account when evaluating the results.

RESULTS AND CONCLUSIONS

The CFD model provided the thermal performance of the discs receiver at different working conditions, with flux densities between 0.6 MW/m^2 and 1 MW/m^2 and air outlet temperatures between 700 °C and 1200 °C. The model also provides the temperature profiles of the discs (Fig. 6) and the air through the receiver (Fig. 7) which enable the full thermal characterization of the receiver.

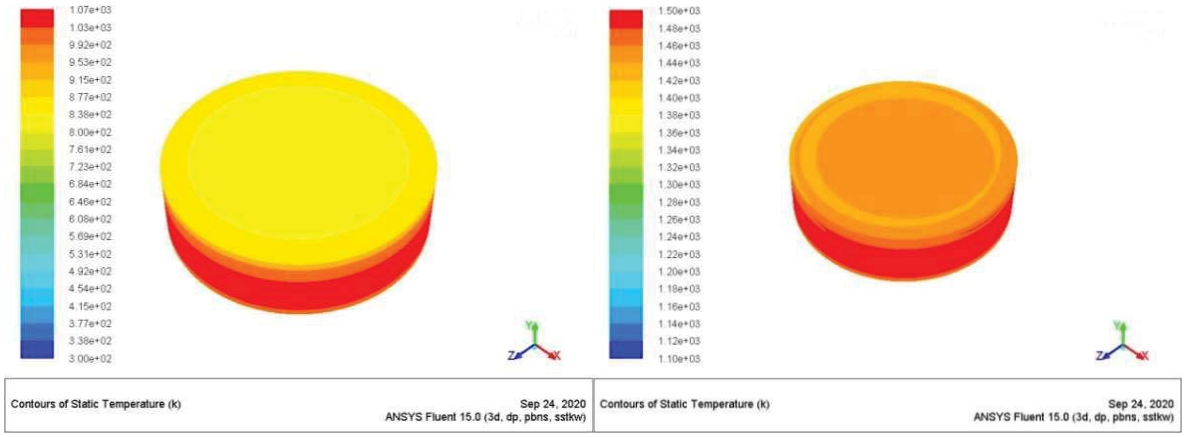

FIGURE 6. Temperature contours of discs (1 MW/m^2)

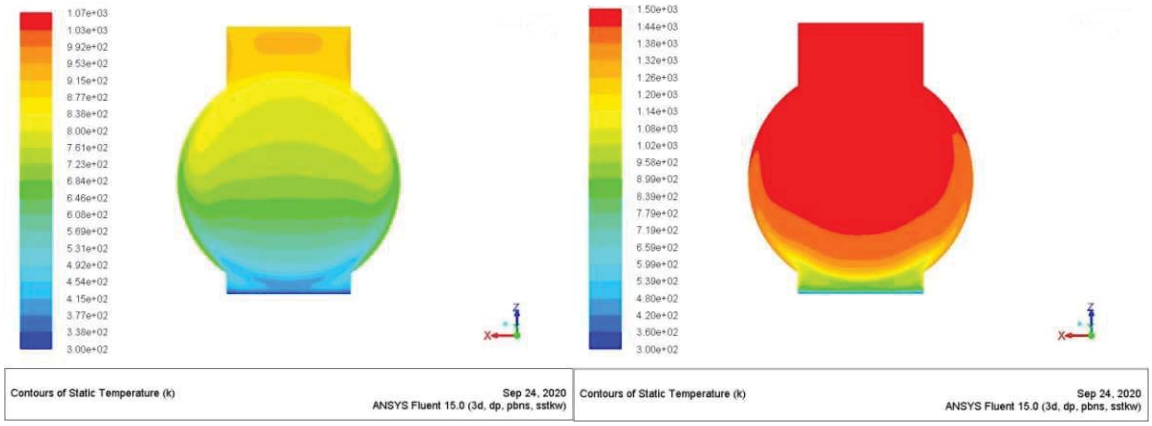

FIGURE 7. Temperature contours of air (1 MW/m^2)

Finally, Fig 8 shows a comparison between thermal efficiencies of foam receiver and discs receiver for different air outlet temperatures and 1MW/cm^2 flux density.

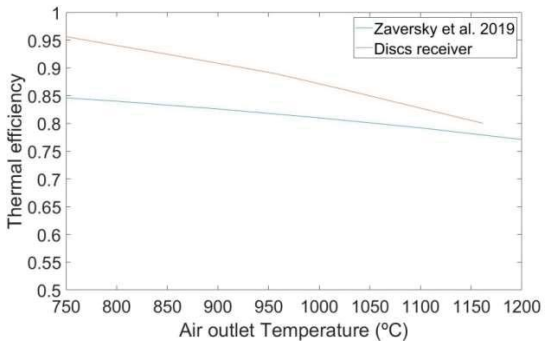

FIGURE 8. Thermal efficiency vs air outlet temperature

It can be seen that the thermal efficiencies of the discs receiver are higher than foam receiver working at the same conditions of solar flux and air outlet temperature.

Comparing the economic and electric results from the plant model after simulating a year of operation, between foam receiver and discs receiver, the LCOE of the plant with discs receiver shows a decrease from 0.135 $/kWh to 0.126 $/kWh. In terms of electrical generation, the receiver discs plant indicates an increase from 1,56799 $x10^8$ kWh to 1,67464$x10^8$ kWh in comparison with the foam receiver plant. However, taking into account the high uncertainty related to cost assumptions and the long-term stability of the complex, high-temperature solar receiver concept, at this stage of development, it is not possible to give a final conclusion regarding the economic viability of the concept. Therefore, forthcoming work of the authors will treat the detailed experimental validation of the rotary disk receiver's simulation results at laboratory scale. In case the promising theoretical results can be confirmed experimentally, the next development stage would be the thorough long-term experimental evaluation at small-scale (cup-level testing) at relevant solar flux boundary conditions.

ACKNOWLEDGMENTS

The authors would like to thank the Government of Navarre for funding this research work under the contract number 0011-1408-2017-000016.

REFERENCES

1. NREL. National Renewable Energy Laboratory, "Assessment of Parabolic Through and Power Tower Solar Technology Cost and Performance Forecast," Golden, Colorado, 2003.
2. Eastman, "Therminol VP-1. Heat transfer Fluid," 2019.
3. R. Bradshaw y R. W. Carling, "A review of the chemical and physical properties of molten alkali nitrate salts and their effect on materials used for solar central receivers," Sandia National Laboratories, Livermore, 1987.
4. M. Romero-Alvarez, E. Zarza, F. Kreith y D. Goswami, *Handbook of energy efficiency and renewable energy*. Boca Raton, USA: CRC Press Taylor and Francis Group, 2007.
5. C. Pabst, G. Feckler, S. Schmitz, O. Smirnova, R. Capuano, P. Hirth y T. Fend, "Experimental performance of an advanced metal volumetric air receiver for Solar Towers." *Renewable Energy* 106 (2017), pp. 91-98.
6. A. L. Ávila-Marín, "Volumetric receivers in Solar Thermal Power Plants with Central Receiver System technology: A review." *Solar Energy* 85.5 (2011), pp. 891-910.
7. F. Gomez-Garcia, J. González-Aguilar, G. Olalde y M. Romero, "Thermal and hydrodynamic behavior of ceramic volumetric absorbers for central receiver solar power plants: A review." *Renewable and Sustainable Energy Reviews* 57 (2016), pp. 648-658.
8. R. Capuano, T. Fend, H. Stadler, B. Hoffschmidt y R. Pitz-Paal, "Optimized volumetric solar receiver: Thermal performance prediction and experimental validation." *Renewable Energy* 114 (2017), pp. 556-566.
9. M. Romero, R. Buck y J. E. Pacheco, "An Update on solar central receiver systems, projects, and technologies." *Journal of Solar Energy Engineering, Transactions of the ASME* 124.2 (2002), pp. 98-108.
10. F. Zaversky, I. Les , M. Sanchez, B. Valentin, J. Brau y F. Siros, "The challenge of solar powered combined cycles-providing dispatchability and increasing efficiency by integrating the open volumetric air receiver technology." *Energy* 194 (2020).

11. F. Zaversky, I. Les, M. Sanchez, B. Valentin, J. Brau, F. Siros, J. McGuire y F. Berand, “Techno-Economic Optimization and Benchmarking of a Solar-Only Powered Combined Cycle with High-Temperature TES Upstream the Gas Turbine.” *De Green Energy and Enviroment*, London, UK, 2019.
12. F. Zaversky, M. Sanchez, M. Roldan, A. Avila-Marin, A. Füssel, J. Adler, M. Knoch y A. Dreitz, “Experimental Evaluation of Volumetric Solar Absorbers - Ceramic Foam vs Innovative Rotary Disc Absorber Concept.” *AIP Conference Proceedings SolarPACES2017*, 2018.
13. ANSYS Inc., *FLUENT-Theory Guide*, Canonsburg: ANSYS, Inc., 2009.
14. S. V. Pantakar, “Numerical Heat Transfer and Fluid Flow.” *Computational Methods in Mechanics & Thermal Sciences*. First ed., New York: McGraw-Hill Book Company, 1980.
15. J. H. Ferziger and M. Peric, “Computational methods for fluid dynamics.” Third ed., Berlin: Springer, 2002.
16. S. Akar, S. Rashidi and J. A. Esfahani, “Second law of thermodynamic analysis for nanofluid turbulent flow.” *Journal of Thermal Analysis and Calorimetry* 132 (2017), pp. 1189-1200.
17. T. P. Dhakal and D. K. Walters, “Curvature and rotation sensitive variants of the K-omega SST turbulence model.” *Proceedings of the ASME 2009 Fluids Engineering Division Summer Meeting* 1 (2009), pp. 2221-2229.
18. H. H. Barbosa Rocha, P. A. Costa Rocha, F. O. Moura Carneiro, M. E. Vieira da Silva and C. Freitas de Andrade, “A case study on the calibration of the k-omega SST (shear stress transport) turbulence model for small scale wind turbines designed with cambered and symmetrical airfoils.” *Energy* 97 (2019), pp. 144-150.
19. F. Menter, “Two-Equation Eddy-Viscosity Turbulence Models for Engineering Applications.” *AIAA Journal* 32.8 (1994), pp. 1598-1605.
20. F. Zaversky, I. Les, P. Sorbet, M. Sánchez, B. Valentin, F. Siros, J. F. Brau, J. McGuire y F. Berard, “CAPTure Concept Specification and Optimization D1.4.” 2020.
21. Thermoflow Inc., “GT PRO- Gas turbine combined cycle design program to create cycle heat balance and physical equipment needed to realize it.” 2011. [On line]. Available: http://www.thermoflow.com/combinedcycle_GTP.html (Accessed 30.4.2013).
22. SimTech-Simulation-Technology, “IPSEpro - Integrated Process Simulation Enviroment.” 2011. [On line]. Available: http://www.simtechnology.com. (Accessed 30.4.2013).
23. W. Short, D. J. Packey y T. Holt, “A Manual for the Economic Evaluation of Energy Efficiency and Renewable Energy Technologies.” 1995.